Published in final edited form as:
Biochemistry. 2012 June 5; 51(22): 4406–4415. doi:10.1021/bi300082s.

Loop Residues and Catalysis in OMP Synthase†

Gary P. Wang[#,‡], **Michael Riis Hansen**[⊥], and **Charles Grubmeyer**[#,*]

[#]Department of Biochemistry and Fels Research Institute, Temple University School of Medicine, 3307 N Broad St., Philadelphia PA 19140

[⊥]Department of Biology, University of Copenhagen, Ole Maaløes Vej 5 DK-2200 Copenhagen N Denmark

Abstract

Residue-to-alanine mutations and a two amino acid deletant have been made in the highly conserved catalytic loop (residues 100-109) of *Salmonella typhimurium* OMP synthase (orotate phosphoribosyltransferase, E.C. 2.4.2.10). As described previously, the K103A mutant enzyme showed a 10^4-fold decrease in k_{cat}/K_M for PRPP; K100A enzyme suffered a 50-fold decrease. Alanine mutations at His105 and Glu107 each gave a 40- and 7-fold decrease in k_{cat}/K_M, respectively, and E101A, D104A, G106A were slightly faster than WT in k_{cat} with minor effects on k_{cat}/K_M. Equilibrium binding of OMP or PRPP in binary complexes was little affected by loop mutation, suggesting that the energetics of ground state binding have little contribution from the catalytic loop, or that favorable binding energy is offset by costs of loop reorganization. Pre-steady-state kinetics for mutants showed that K103A and E107A had lost the burst of product formation in each direction that indicated rapid on-enzyme chemistry for WT, but that the burst was retained by H105A. Δ102Δ106, a loop-shortened enzyme with Ala102 and Gly106 deleted, showed a 10^4-fold reduction of k_{cat} but almost unaltered K_D values for all four substrate molecules. The 20% (i.e. 1.20) intrinsic [1′-^{3}H]OMP kinetic isotope effect (KIE) for WT is masked because of high forward and reverse commitment factors. K103A failed to express intrinsic KIEs fully (1.095 ± 0.013). In contrast, H105A, which has lesser catalytic lesion, gave a [1′-^{3}H]OMP KIE of 1.21 ± 0.0005 and E107A (1.179 ± 0.0049) also gave high values. These results are interpreted in the context of the X-ray structure of the complete substrate complex for the enzyme (*1* preceding paper). The full expression of KIEs by H105A and E107A may result from a less secure closure of the catalytic loop. The lower expression of KIE by K103A suggest that in these mutant proteins the major barrier to catalysis is successful closure of the catalytic loop, which when closed, produces rapid and reversible catalysis.

Introduction

OMP synthase (orotate phosphoribosyltransferase, E.C.2.4.2.10), like other members of the Type I PRTase evolutionary family, is notable for the prominent peptide loop adjacent to the active site. This loop is highly flexible in its open state, and is not visualized in electron density maps for some OMP synthase structures (1-4). For catalysis to occur, the loop from one subunit must descend to cover the active site formed by the adjacent subunit (5). In its down position, as described for the yeast enzyme by Gonzalez-Segura et al. (6), and for the *S. typhimurium* enzyme in the preceding paper (1), the loop forms a pair of anti-parallel β-strands, and loop residue B-factors resemble those for bulk protein atoms. Five new

†This research was supported by a grant from the National Institutes of Health (GM48623 to C.G.).

*Address correspondence to this author: Telephone 215-707-4495, ctg@temple.edu.
‡Current address: Department of Medicine, University of Florida 1600 SW Archer Road Gainesville, FL 32610 Gary.Wang@medicine.ufl.edu

interatomic contacts form within the loop, between the loop and the remainder of the protein, and between the loop and bound ligands. Previously, we measured loop dynamics using NMR and found that loop movement from open to closed occurred with a rate of about 12,000 s^{-1} when PRPP occupied the active site, and that loop opening in this complex occurred at about 400 s^{-1} (7).

Loop movements are recognized as an integral part of chemical catalysis by enzymes (8). One archetype for loop movement is TIM, whose loop moves as a rigid body to occlude the active site and prevent an alternative net elimination reaction from the ene-diol intermediate (9). In that case, solid state NMR indicated that loop movement rates are not affected by occupancy of the active site, suggesting that loop movement is not gated by substrate (10). In other enzymes, loop movement proceeds from an unstructured loop-open form, to one that becomes structured over the active site. This is the case in GPAT (11) and HGPRTase (12), two Type I PRTases, both of which show highly structured “closed” forms of the loop, which also capture and immobilize bound water molecules, and relatively unstructured “open” forms. In OMP synthase, as shown in the preceding paper, loop closure also is a reordering event rather than rigid-body motion about a hinge. For this type of movement to occur, there must be a dynamic energetic balance between the energy-demanding events of peptide ordering, and the energy-yielding formation of intra-loop, loop-core and loop-ligand hydrogen bonds. The 30:1 equilibrium of closed to open forms in binary E•MgPRPP complexes (7) suggests that the balance is only slightly in favor of loop closing, in keeping with the enzyme's need to reopen to release products. Interactions that favor or disfavor each of the loop-open and loop-closed states will be important in determining the equilibrium between them. As yet, we have been unable to observe residue interactions in the loop-open state.

In OMP synthase, loop residues are known to be essential for catalytic chemistry (5, 13), and loop movement is thus responsible for recruiting these essential residues to the active site. Several chemical roles could be proposed. In the forward direction, proton transfer to leaving pyrophosphate could minimize accumulation of negative charge. Although the pKa for PP_i is only 9 (14), protonation may provide slight assistance. At the α-phosphate position, Lys26, His105 and Lys103 could each perform proton transfer. Protonation may not be necessary, in that positive charges provided by side chains and metal ions may also neutralize some of the developing electron density on leaving PP_i. To some extent this is clearly the case, since the loop-closed active site surrounds the pyrophosphate moiety with positive charges from Lys103, Lys100, Arg99, and Lys26. A second mode of catalytic participation would be for loop residues to participate in geometric stabilization of the transition state, promoting the straight line geometry of incoming and leaving ligands about C1 of PRPP and OMP (15, 16).

It is also clear that large motions of bound substrates occur leading up to transition state formation. As discussed in the preceding paper (1), a 7 Å movement of the ribosyl C1 is noted between its position in OMP and PRPP complexes, and the preceding paper suggested that 1-2 Å of additional movement of C1 remains to be achieved. It appears that as the loop undergoes its major closing movement, the bound substrates move into position for catalysis.

One can inquire as to the degree of coupling between movement and chemistry. Bulk loop movement in OMP synthase is relatively slow (values of 10^2-10^4 Hz were recorded by Wang et al. (7) for overall opening and closing) compared to bond vibration frequencies (10^{12} Hz) that govern the lifetime of transition states. This eight order-of-magnitude difference in rates suggests that coupling would be impossible. However, the transition state involves a suite of atoms contributed by both the substrate and the protein. In a completely

concerted mechanism, the transition state proper would be achieved as movement of atoms from the bound substrate and from the loop permitted the formation of intra loop, loop-core, and loop-transition state hydrogen bonds. To the extent that these final movements could be achieved only at the culmination of the bulk motion of the loop, then the enzyme would efficiently direct bulk loop motion into the reaction coordinate motion required for catalysis. An alternative view is that the final steps of loop movement set up a relatively long-lived (i.e. nsec-msec) state within which random thermal movements allow for achievement of the transition state. An analysis of hydrogen/deuterium amide exchange rates in HGPRTase (17) showed that a complex of that enzyme with a transition state analog slowed exchange of loop (and non-loop) amide protons far more efficiently than an equilibrating Michaelis complex, suggesting specific and widespread structural stiffening at or near the transition state itself.

Few techniques allow us to view protein dynamics in the high frequency or small distance range demanded by the transition state. One technique available to enzymologists is that of competitive kinetic isotope effects (KIE). In competitive KIE measurements, we obtain a ratio that expresses the relative success rates of different isotopically labeled substrates in traversing the transition state barrier. This ratio is partly governed by the transition state structure, which causes less efficient catalysis with a particular labeled substrate. When a Michaelis complex that has embarked along the reaction coordinate encounters the energy barrier imposed by the transition state, it may either traverse it, or fall back to its ground state. If escape of the labeled substrate is allowed, the enzyme will discriminate against the heavy-atom label. If escape is not allowed, no KIE will be expressed. In OMP synthase, loop closure appears to physically block the egress of bound substrates from the active site. Thus, loop opening would be required for a KIE to be observed. If loop closure precedes transition state formation then we would expect that mutants with slow on-enzyme chemistry (i.e. a high barrier for the chemical transition state) would allow for relatively frequent loop-opening on bound complexes, allowing full expression of the KIE. In a similar way, mutants that have rapid chemistry would not express a KIE. KIE studies have been carried out on several enzymes with mobile elements and support the close relationship between movement and catalysis (18-20).

In this study we have mutated each of the residues of the catalytic loop of *S. typhimurium* OMP synthase. The mutant enzymes show a range of catalytic lesion, from slight increases in k_{cat} to a 10^5-fold reduction. Chemical quench experiments allow us to measure rates of on-enzyme chemistry. When KIE experiments are performed with these mutant enzymes, several show unexpected behavior.

Materials and Methods

Materials

[2-^{14}C]orotic acid was a product of Moravek Biochemicals, Inc. (Brea, CA). [γ-^{32}P]ATP was from Amersham. [^{32}P]PP_i was from Dupont NEN Research Products. Thin layer chromatography plates of polyethyleneimine cellulose were obtained from Alltech (Deerfield, IL). Yeast inorganic pyrophosphatase was purchased from Boehringer-Mannheim Corp. Inorganic chemicals and chromatography solvents were purchased from Fisher. Mutagenic primers were synthesized by Ransom Hill Bioscience, Inc. Materials for mutagenesis and DNA sequencing procedures were purchased from U.S. Biochemicals and New England Biolabs Inc. DTT was from U.S. Biochemicals. Buffers, orotic acid, PRPP, OMP, amino acids, other reagent grade biochemicals, and bacterial culture media were obtained from Sigma. Sephadex G-50 resin was from Pharmacia.

Synthesis of Radiolabeled Substrates

[2-^{14}C]OMP was prepared from [2-^{14}C]orotate using OMP synthase (21). [β-^{32}P]PRPP was prepared from [γ-^{32}P]ATP using PRPP synthase (a gift of Dr. Robert Switzer) as previously described (22). [5-^{32}P]PRPP was also prepared enzymatically. [γ-^{32}P]ATP (40 μCi) was incubated with 200 μM ribose, 3 mM $MgCl_2$, 5 mM phosphoenolpyruvate, 25 units ribokinase, and 10 units pyruvate kinase in 200 μL 50 mM potassium phosphate, 50 mM Tricine, pH 8, at 30°C for 1 hr. Ribokinase and pyruvate kinase were then removed from the reaction mixture using a Centricon-10 apparatus. ATP was removed using a 1 mL column of charcoal/Whatman CF11 cellulose (1:4) and ribose 5-phosphate was eluted with 50 mM potassium phosphate at pH 8.0. The two 1 mL fractions containing [5-^{32}P]ribose 5-phosphate were incubated with 4.4 mM ATP, 4.4 mM $MgCl_2$, 10 μg pyruvate kinase, 2.2 mM phosphoenolpyruvate, 1 unit rabbit muscle adenylate kinase, and 1 flake (about 0.1 mg) of freeze-dried PRPP synthase for 30 min at 30°C. Enzymes and ATP were removed as above. The fractions from the charcoal column containing [5-^{32}P]PRPP were pooled and applied to a Mono-Q column (Pharmacia 0.5 × 5 cm). The column was eluted at 1 mL/min with a 60 mL linear gradient of 0-1 M NaCl in 20 mM sodium phosphate pH 7.4. The fractions containing radiolabeled PRPP were detected by Cerenkov radiation in a liquid scintillation counter, pooled, aliquoted, and stored at −80°C until use.

[1-^{3}H]PRPP was prepared from [1-^{3}H]ribose (Moravek) using ribokinase and PRPP synthase in a single reaction mix. Reactions (1 mL) contained 3.3 mM ATP, 1 mM $MgCl_2$, 100 μM ribose, [1-^{3}H]ribose, 10 μg pyruvate kinase, 2.5 mM phosphoenolpyruvate, 1 unit rabbit muscle adenylate kinase, 25 units ribokinase. One flake of PRPP synthase was added, and reaction allowed to continue at 30°C for 60 min. Enzymes and ATP were removed, and the labeled PRPP was purified as described above for [5-^{32}P]PRPP. For synthesis of [4, 5-^{14}C]PRPP, [5, 6-^{14}C]glucose (American Radiolabeled Compounds; 60 mCi/mmol) was used as the precursor in a single reaction taken from Li (23). Reaction mixtures (1 mL) in 50 mM potassium phosphate pH 7.8, contained 10 mM $MgCl_2$, 1 mM ATP, 10 μCi [5,6-^{14}C]glucose, 20 mM phosphoenolpyruvate, 5 mM NADP, 10 mM α-ketoglutarate, and 5 units yeast hexokinase, 1 unit rabbit muscle pyruvate kinase, 5 units yeast glucose 6-phosphate dehydrogenase, 0.5 units yeast 6-phosphogluconate dehydrogenase, 1 unit Torula phosphoriboisomerase, 1 flake PRPP synthase, and 1 unit beef liver L-glutamate dehydrogenase. Precipitated ammonium sulfate suspensions used for pyruvate kinase and glutamate dehydrogenase provided sufficient ammonium ion for the glutamate dehydrogenase reaction. After reaction, enzyme protein was removed by a Centricon device, and the PRPP purified by chromatography on Mono-Q as above.

[1′-^{3}H]OMP and [4′, 5′-^{14}C]OMP were prepared from the cognate labeled and purified PRPP molecules using OMP synthase. Reaction mixtures (1 mL) in 50 mM potassium phosphate, pH 7.4, contained 6 mM $MgCl_2$, 0.3 mM orotate, 2 units yeast pyrophosphatase, and labeled PRPP (5 μCi). The reaction was started by addition of 20-50 μg of K26A OMP synthase, previously dissolved in the same buffer. After 30 min at 30°C, enzymes were removed by Microcon device, and the OMP purified by Mono-Q chromatography as for PRPP, except that a 120 mL gradient was employed.

Construction and Purification of OMP Synthase Loop Mutants

A silent mutation 5′ of the loop coding sequence generated using overlapping PCR (24) introduced a *Bgl*II site. This *Bgl*II restriction site and a naturally occurring *Bss*HII site 3′ of the loop coding sequence enabled insertion of PCR fragments encoding any desired loop sequence. A 1 kbp *Eco*RI-*Pst*I fragment from pCG13 (25) encoding the entire *pyrE* gene of *S. typhimurium* OMP synthase was used as the template. Oligonucleotide primers used were 5′CACGATAAAGATCTGCCGTACTGC 3′ and

5′GCAGTACGGCAGATCTTTATCGTG 3′. The 0.7 kbp PCR product, containing the new *Bgl*II site, was digested with *Nde*I and *Bam*HI, and ligated with T7 promoter vector pRSET C (Stratagene) previously digested with *Nde*I and *Bgl*II, yielding pGW01. The entire coding sequence was subjected to DNA sequencing.

To construct the loop mutants, overlapping PCR was similarly employed using pGW01 as a template. Oligonucleotide primers for the mutagenesis procedures are listed in Table 1. To minimize subsequent DNA sequencing, the 0.7 kb PCR product carrying the mutation was digested with *Bgl*II and *Bss*HII, and the 68 bp fragment was ligated with pGW01 previously cut with the same restriction endonucleases, resulting in a recombinant plasmid carrying the mutation in the coding sequence. All desired mutations were confirmed by DNA sequencing of the 68 bp insert.

To overexpress WT and mutant OMP synthase, the recombinant plasmid was transformed into *E. coli* host BL21(DE3). Both WT and mutant constructs produced a high level of expression. Enzymes were purified from 6 L cultures using the protocol described in Bhatia et al. (25) with modification (26), except that 0.1 mM phenylmethanesulfonyl fluoride (PMSF) was added to the cells immediately prior to sonication. Approximately 200-250 mg of highly homogeneous OMP synthase was typically isolated from 20 g of cells.

Enzyme preparation

OMP synthase mutant proteins were prepared using the procedure described previously for the WT enzyme (13) and were highly homogeneous. Prior to enzymatic assays, enzymes stored in 65% saturation $(NH_4)_2SO_4$ at 4°C were centrifuged and desalted using centrifuge columns (27) . The revised extinction coefficient of 0.51 for a 1mg/mL solution at 280 nm (21) was used throughout this work. The molecular weight of the enzyme 23,561 (28) was used to calculate molarity of enzyme subunit.

Enzyme Assays

Pyrophosphorolysis of OMP (the standard reverse OMP synthase reaction) was monitored in the thermostatted cuvette holder of a spectrophotometer as an increase in absorbance at 302-304 nm as previously described (26). The standard forward reaction using orotate and PRPP as substrates was monitored as a decrease in absorbance over the same wavelength region. Buildup of inhibitory OMP limits the extent of the linear portion of progress curves. For each assay, the buffer mixture was allowed to reach thermal equilibrium in a 30°C dry bath before addition of substrates followed by 0.05-0.1 μg of WT enzyme. For the less active mutant OMP synthases, the quantity of enzyme was increased as needed in order to produce measurable linear initial rates. One unit of activity was defined as the amount of enzyme needed to convert 1 μmol of orotate to OMP (or 1 μmol of OMP to orotate) per minute at 30°C. For the calculation of k_{cat}, the subunit Mr was employed as noted in the legends Tables and Figures.

Steady-state kinetic experiments were conducted for WT and mutant enzymes by monitoring absorbance changes at 302-304 nm at 30°C in both the forward phosphoribosyltransferase and the reverse pyrophosphorolysis reactions (13). Assay mixtures for the forward reaction contained 75 mM Tris-Cl, 6 mM $MgCl_2$, pH 8.0, and 10-300 μM orotate at 1 mM PRPP, or 20-1000 μM PRPP at 300 μM orotate in 1.0 mL final volume. For the reverse reaction, assay mixtures were composed of 80 mM Tris-Cl, 3 mM $MgCl_2$, pH 8.0, and 1.5-100 μM OMP at 2 mM PP_i, or 20-2000 μM PP_i at 100 μM OMP in the same final volume. The use of 0.05-0.1 μg WT or of 0.05-50 μg mutant OMP synthase provided quantifiable linear initial rates for the calculation of kinetic parameters. All kinetic data were analyzed as described previously (25), and K_M and V_{max} are reported with their standard errors.

Equilibrium Binding

For the binding of PRPP, OMP, orotate, and PP_i, a centrifugal filtration method using Centricon-10 or Microcon-10 apparatus (Amicon) was employed (21). The buffer was 80 mM Tris-Cl or Na-Tricine, pH 8.0, in the presence of $MgCl_2$ (3-15 mM, as noted). All binding data were subsequently fit to a single site model using UltraFit (Biosoft). K_D and n values are reported.

Chemical Quench Experiments

Pre-steady-state analyses for selected OMP synthase mutants were performed in an Update Instruments (Madison, WI) Precision Syringe Ram, Model 1010, equipped with a grid-type mixer, following the protocols described previously for the WT enzyme (21). For the analysis of the reaction kinetics in K103A, E107A, and H105A, concentrations of the reaction components are given in the legends to the Figures. Reactions quenched in 0.9 N perchloric acid were centrifuged to remove denatured protein, neutralized with 6 N KOH, and chilled on ice. $KClO_4$ precipitate was removed by centrifugation and the samples stored at −20°C overnight. Prior to the chromatographic analysis, the reaction mixtures were thawed on ice, and additional $KClO_4$ precipitate was again removed by centrifugation. A sample of the supernatant (200 μL) was applied onto an anion exchange column (0.4 × 25 cm; Alltech or ISCO SAX, 5 μm) with isocratic elution at 1 mL/min in 20 mM Na-phosphate, pH 6.1. Under these conditions, OMP elutes at 8 min, and orotate elutes at 3.5-5 min. Radioactive orotate and OMP were quantitated by liquid scintillation counting.

Kinetic Isotope Effects

For the forward reaction, 1.0 ml mixtures contained 50 mM potassium phosphate buffer, pH 7.4, 3 mM $MgCl_2$, 0.6 mM orotate, 1.5 units yeast OMP decarboxylase (Sigma product O-9251), 2 units of yeast inorganic pyrophosphatase (Boehringer product 108987) and 100 μM PRPP, containing about 10,000 cpm each of [1-^{3}H]PRPP and either [5-^{14}C]PRPP or [5-^{32}P]PRPP. Reactions were initiated by the addition of enzyme and preceded for 20-30 min at 30°C, using a quantity of WT or mutant OMP synthase sufficient to produce about 50% conversion of labeled PRPP to OMP, an extent of conversion which gives optimal accuracy in quantitating KIE values from remaining substrate (29). For every experiment a separate reaction was performed in which no enzyme was added (designated 0% reaction) and one in which 0.25 mM hypoxanthine and 200 μg of human HGPRTase were present (100% reaction). Two 50% conversion reactions were run. Reactions were terminated by the addition of EDTA, pH 8.0, to 50 mM final concentration (resulting in 1.1 mL), a 0.05 ml sample was taken to determine the total cpm and 1.0 ml of the remaining mixture was applied to columns (5-6 cm in pasteur pipettes plugged with glass wool) of Whatman CF11 cellulose: activated charcoal (4:1, w:w), previously equilibrated with 50 mM potassium phosphate pH 7.4. Three 1 ml washes with 50 mM potassium phosphate, pH 7.4 were used to produce a total of 4 fractions, collected in Research Products International 20 ml glass scintillation vials. To each fraction was added 15 ml of ICN Eco-Lite(+) liquid scintillation cocktail. The contents of the vials were mixed, and the radioactivity in each was measured using a Beckman LS6500 liquid scintillation counter. The dual-channel program employed was uncorrected for quenching. Separate determinations verified that no spillover from the ^{3}H channel into the ^{14}C channel occurred, and quantitated the spillover of counts from ^{14}C into the ^{3}H channel. The complete sequence of vials for each entire experiment was counted 10 times. In some cases, the first several rounds of counting appeared to show minor luminescence (anomalously high or erratic ^{3}H/^{14}C ratios) and the data were rejected. Data from each count cycle were analyzed by separately summing ^{3}H and ^{14}C radioactivity from those background-corrected fractions that contained radiolabel from remaining PRPP, typically fractions 2 and 3. Comparing the 50% conversion radioactivity with that for 0% (which typically contained 1-2% of the expected radioactivity for each isotope) and 100%

(which typically contained 98-101% the expected radioactivity for each isotope) allowed an accurate calculation of the percent conversion of each isotopically labeled PRPP to OMP. In most experiments the 0% and 100% values for the entire series of 10 count cycles were averaged and the mean value used for the calculation of the individual KIEs in the next step. The equations given by Parkin (29) were used in a computer spreadsheet used to calculate the KIE for each count cycle. The mean of all the KIE values for the 10 cycles was calculated, together with the standard deviation. Data from two to five experiments was averaged and a standard deviation calculated. Low standard deviations within an experiment, and reproducibility, were critically dependent on several of the procedures employed here, including the use of glass vials, high quality cocktail, and the use of repeated count cycles.

For the reverse reaction, the procedure differed in only a few respects. Reactions (1 ml) contained 50 mM potassium phosphate, pH 7.4, 3 mM $MgCl_2$, 0.25 mM $NaPP_i$, 100 μM OMP with no coupling enzymes present. The radioactive label was a mixture of [1′-^{3}H]OMP and [5′-^{14}C]OMP. Reactions (20-30 min) were set up to give 25-30% conversion of OMP to PRPP. A 0% conversion sample contained no enzyme, and a 100% conversion was performed with WT OMP synthase. Sample work-up and calculations were identical to those above.

Results

Site-directed Mutagenesis of Surface Loop Residues

Comparison of sequences among *pyrE* genes encoding OMP synthase reveals a high degree of sequence conservation in the region between Arg99-Gly109. Identification of the conserved surface mobile loop prompted us to investigate the catalytic roles of individual loop residues by alanine scanning (30). A deletion mutant, designated Δ102Δ106, was also constructed in which two residues, Ala102 and Gly106, that flank the catalytically essential Lys103 were removed.

Expression and Purification of Mutant OMP Synthases

All mutant constructs produced high levels of expression in BL21(DE3) *E. coli*, and gave large quantities of highly purified enzyme. No stability problems were noted with any of the mutant enzymes.

Steady-State Kinetics of Loop Mutants

Steady-state kinetic parameters were determined for each loop mutant (Tables 2 and 3). Previous data for K100A and K103A (13) are included for comparison. The most dramatic effect on enzymatic activity upon alanine substitution was observed in the K103A mutant. The k_{cat} values for the forward and reverse reactions decreased 1000- and 350-fold relative to the value for WT, respectively. The catalytic efficiency, k_{cat}/K_M, for each of the four substrates was also severely decreased.

The smaller changes in the steady-state kinetic parameters for the E107A mutant paralleled those of K103A. The k_{cat} values for the E107A mutant showed a 23- and 60-fold decreases for the forward and reverse reactions. The k_{cat}/K_M value for PP_i decreased 600-fold, whereas that for OMP dropped 250-fold relative to the WT value. The mutation also produced a 500-fold decrease in the catalytic efficiency for orotate, whereas the value for PRPP decreased only 7-fold.

Alanine substitution at Lys100 produced mild (1.5- and 5-fold) changes in the steady-state k_{cat} values, but more pronounced effects (5-50-fold decreases) on the k_{cat}/K_M values.

The H105A mutant enzyme suffered a 10-fold decrease in k_{cat} values in each direction. The k_{cat}/K_M values displayed 20-200-fold decreases. The G109A mutant showed 1.5- and 2-fold decreases in k_{cat}, and 3-30-fold decreases in k_{cat}/K_M. Alanine substitution at Glu101, Asp104, or Gly106 resulted in no change (G106A) or even slight increase (E101A and D104A) in activity. In these mutants, only small changes (less than 5-fold) in the k_{cat}/K_M values were observed for each of the four substrates.

Equilibrium Binding Measurements

The K_D values for OMP and PRPP for the mutant enzymes (Table 4) showed few significant effects. D104A showed tighter binding of PRPP.

Pre-Steady-State Analysis

Pre-steady-state kinetics on the WT enzyme showed that overall forward or reverse catalysis proceed with a rapid (>300 s^{-1}) on-enzyme chemistry followed by a slower step involving product release through loop opening and partitioning between loop reclosure and product release (7, 21). Mutants in which on-enzyme chemistry is no longer fast relative to the release of products should fail to show pre-steady-state bursts, whereas a burst of product formation is expected if product release remains rate-limiting

K103A showed no evidence of pre-steady-state burst (Figure 1). In the forward reaction at 22°C, the steady-state rate was 0.02 s^{-1}, comparable to the k_{cat} value (0.05 s^{-1}) determined at 30°C. These results appear to indicate that K103A undergoes a rate-limiting on-enzyme step that could be phosphoribosyl transfer chemistry, or a step preceding it.

For the E107A mutant in which a significant reduction in the k_{cat} value was observed, the chemical quench analysis in the reverse reaction showed no pre-steady-state burst of orotate formation (Figure 2). The steady-state rate was 0.4 s^{-1}, comparable to the k_{cat} value determined at 30°C (0.3 s^{-1}).

For the H105A mutant, transient kinetics experiments performed in the forward and reverse reactions revealed pre-steady-state bursts of OMP formation followed by a slower steady-state phase (Figure 3, reverse reaction not shown). The pre-steady-state phase was fit to a rate constant of 200 s^{-1}. The magnitude of the burst was 0.64 ± 0.08 mol [^{14}C]OMP/mol enzyme dimer. The steady-state phase (6.4 s^{-1}) was comparable to the k_{cat} value (5.3 s^{-1}) determined spectrophotometrically at 30°C. Thus catalysis in the H105A mutant, like that of the WT enzyme, proceeds with a relatively rapid on-enzyme chemistry followed by a slow step, probably associated with the overall product release process.

Δ102Δ106, A Loop-Deleted OMP Synthase

The deletion mutant, Δ102Δ106, suffered the largest decrease in the values of k_{cat}: 56000-fold and 29000-fold for the forward and the reverse reactions, respectively. The marked reduction in the k_{cat} values for Δ102Δ106 emphasize that the loop is extremely important, although not absolutely essential. The equilibrium binding constants (K_D) for all four ligands are shown in Table 5. Only minor changes in the K_D values for PRPP and OMP were noted.

Kinetic Isotope Effects Studies

Competitive kinetic isotope effects provide a view of the transition state (31). The use of the slowly utilized substrate phosphonoacetate allowed measurement (15, 16) of an intrinsic [1′-^{3}H]OMP KIE of 1.20 for the reverse reaction, which together with other KIE values led to the structure of an oxocarbenium-like transition state for group transfer. Such S_N1-like transition states are very frequent among ribosyl transfers (32) and uniformly give rise to

similarly significant intrinsic [1-^{3}H] α-secondary isotope effects. In this work, the transition state structures for mutant enzymes were not determined, and were assumed to be similar to WT. This assumption may be incorrect, in that mutation, of key residues or even at remote sites, has been shown to alter transition state structure (20, 33). In addition to the intrinsic KIE, three other components determine observed competitive KIE values. The forward and reverse commitment factors c_f and c_r (31) quantitate the extent to which the labeled substrate and product have opportunity to dissociate from complexes that are in equilibrium with the transition state. Finally, the isotopic equilibrium constant ($^TK_{eq}$) for the isotopically sensitive step also participates. In OMP synthase both forward and reverse commitment factors for KIE experiments using PRPP and OMP are substantial and mask intrinsic KIEs. Any change that lessens these commitments will allow the expression of intrinsic KIEs. Since movement of the flexible loop is essential for closing the active site, and for either subsequent or concerted development of the transition state, it was of interest to determine the observed KIE for loop mutants.

For conversion of OMP to PRPP, the competitive KIE (29) method measures enrichment of ^{14}C over ^{3}H in the product PRPP. For the forward KIE using [1-^{3}H]PRPP, what is measured is enrichment of ^{3}H over ^{14}C in the remaining PRPP. In each case a trapping system (PP_iase or OMP decarboxylase) was used to capture one released product and render the net reaction irreversible.

KIE data are presented in Table 6. For WT, the observation of a modest 1.059 ± 0.004 KIE in the reverse reaction duplicates values determined (15, 16), and the [1′-^{3}H]PRPP value of 1.019 ± 0.007 is that expected for the high commitment factors for that substrate. G106A and D104A also show low KIEs. However, the behavior of H105A differs: the value of 1.21 ± 0.005 for [1′-^{3}H]OMP is identical to the intrinsic KIE measured earlier (15, 16), and the value of 1.136 ± 0.0071 for [1-^{3}H]PRPP is the highest of any of the values seen here. In a similar, although less pronounced fashion, the reverse reaction for E101A, and both reactions of E107A also show pronounced KIE values.

More surprising was the finding that K103A, the slowest single point mutant, gave a WT-like KIE in the forward direction, and a 1.095 ± 0.013 KIE in the reverse. This latter measurement was repeated many times, and special caution was taken to avoid contamination with WT *E. coli* enzyme.

Discussion

Our findings here can be discussed in two parts. First, it is clear that several loop residues are important to the OMP synthase reaction, and that these residues must exercise their function in loop-closed complexes. Secondly, loop mutation produced a somewhat unexpected pattern of KIE effects, which may provide insights into the role of loop residues in catalysis.

Our previous chemical modification and mutagenesis studies of Lys100 and Lys103 revealed that these residues were important (13, 26). For Lys100, the structure of the asymmetric loop-closed enzyme (1, 6) revealed a potential role in inter-subunit communication. Ground state binding of PRPP and PP_i are both affected with 1.5-5-fold decreases in k_{cat}.

Lys103 is clearly more important to catalysis. K103A suffered 2000-15000-fold decreases of k_{cat}/K_M in both directions. The mutant enzyme also has slow on-enzyme chemistry, as revealed by pre-steady-state kinetics. Given the formation of three hydrogen bonds to the α- and β-phosphates of PRPP in the closed structure (1, 6), Lys103 appears poised to provide geometric stabilization, proton transfer or charge neutralization at the transition state. This

interaction is only of moderate importance in the binary complex with MgPRPP, where a 4-fold increase in K_D was recorded, or with OMP, whose K_D was unchanged by the mutation.

From the position of His105 at the tip of the loop, and its relatively high degree of conservation among OMP synthases (in bifunctional UMP synthases His105 is replaced with tyrosine), it appeared that this residue might have an essential role in catalysis. The structure of the loop-closed form (1, 6) suggests a direct role for His105 in binding to the α-phosphate, perhaps protonation/deprotonation of the leaving/attacking pyrophosphate. H105A enzyme preserved a catalytic burst in pre-steady-state chemical quench experiments with 10-fold reduction in k_{cat}. Binding of PRPP and OMP in binary complexes was little affected by the mutation.

Since Lys103 was the most critical residue, we sought to alter its position in the complete Michaelis complex by removing flanking residues Ala102 and Gly106 to produce Δ102Δ106. From the WT structure, it is likely that three hydrogen bonds from Lys103 to PRPP, and one from His105 to PRPP will be lost, as well as intra-loop hydrogen bonds between the Lys103 peptide nitrogen and the Gly109 carbonyl oxygen, between Lys103 ε-amino and the carboxylate of Glu107 and between the His105 carbonyl oxygen and Gly108 peptide nitrogen. One would predict that the closed loop of Δ102Δ106 would be far looser in structure than WT, and would need to deform if Lys103 and His105 of the truncated loop are to reach the α-phosphate of PRPP. This mutant was severely crippled, suffering a 10^5-fold reduction in k_{cat}, suggesting the interactions of Lys103, and perhaps His105 in stabilizing the transition state are worth up to 6.4 kcal/mol.

Glu107 also participates in hydrogen bonds that appear to be important for productive loop closing, including a 2.7 Å bond to the ε-amino of Lys103 and a 2.7 Å interaction with the ε-amino of Lys73 provided by the other subunit of the dimer. In E107A, k_{cat} values were correspondingly reduced by 25-60-fold, and k_{cat}/K_M values were reduced by 7-500-fold.

The behavior of some of the other loop residues is puzzling. Asp104 makes no interactions that can be seen in loop-closed structure. However, the residue is well conserved, being replaced by alanine in a few bifunctional UMP synthases. Kinetic data show that the D104A enzyme is slightly faster than WT, with minor decreases in k_{cat}/K_M values. We note that Asp104 is on the interface of the two open loops of previous structures (e.g. 1OPR, *3*), and although side chains were too mobile to be assigned in those complexes, it may be that Asp104 from one loop and Lys103 of the other loop can pair to stabilize the loop-open conformation of the dimer.

Like D104A, E101A was reproducibly faster in catalysis than WT, with no change in K_D for PRPP, and a 4-fold increase for OMP. No hydrogen bonds, other than a long backbone amide bond to Arg99, can be seen in the loop-closed structure. It again appears that loop-open structures may prove of more value in revealing the role for Glu101.

The picture we get from the catalytic effects of loop mutation is that loop residues may be responsible for a considerable contribution to catalysis, stabilizing the transition state by about 6 kcal/mol. The simple and naive way to think about this stabilization is that loop movement and chemistry are concerted processes: substrates bind to an open active site, then as the loop closes, ligand movement and residue movement occur, and reach their culmination as the transition state is reached. What is pleasing about this proposal is its continuous nature: once loop closure begins, there is no reason why it should stop until opposing steric forces or the height of the combined motional and chemical transition state barrier stop it. This kind of coupling contains the idea that the chemical barrier to catalysis is only one component of the many bonding interactions that change as the motion reaches its culmination. What is less pleasing about this proposal is the rates of events. Since overall

loop closing may occur at 12000 s^{-1} (7), but the lifetime of a transition state is less than that of a bond vibration, 10^{-12} s, this analysis is clearly limited.

Another analysis suggests that the ligand-bound loop-open state is followed by a discrete loop-closed intermediate, like that described in the crystal structure. In this state, catalysis awaits minor adjustments of residues to occur in the transition state. This model resembles the “near attack conformers” (NACS) proposed by Bruice and Benkovic (34). Since we can observe such a loop-closed state in the crystal structure, it is clearly achievable.

One way to look at the relative energetics of the chemical transition state barrier and the loop-open state is through KIE experiments. The basic equation for translating an on-enzyme (intrinsic) isotope effect (i.e. the magnitude of the effect of isotopic substitution on the rate constant for crossing the transition state barrier at which the isotope effect occurs, designated ^{3}k in this case) into an observed competitive KIE is

$$KIE=\left[\left(^{3}k\right)+c_f+c_r\left(^{3}Keq\right)\right]/(1+c_r+c_f)$$

(35). If ^{3}Keq, the isotopic equilibrium is assumed to be close to one, the equation simplifies to:

$$KIE=\left[\left(^{3}k\right)+c_f+c_r\right]/(1+c_r+c_f)$$

in which c_f and c_r are “commitment factors” that represent the partitioning of bound substrate between net forward catalysis and dissociation (c_f) and of bound product between dissociation and re-crossing of the transition state barrier, c_r. Here, we make an assumption that the transition state, and thus ^{3}k, will remain relatively constant among the mutant enzymes, and that only alterations in commitment factors have changed. Since the origin of the 1.20 ^{3}k for OMP synthase is the oxocarbenium-ion character of the transition state, which is in large part a result of the character of the ribosyl substrates, this is likely. However, it may be that in the absence of key residues to generate or stabilize the oxocarbenium-like transition state, the transition state itself becomes more Sn2-like, with a [1-^{3}H] ^{3}k approaching 1. This outcome has been observed for the humane purine nucleoside phosphorylase, even with remote mutation (20, 33). No further experiments were undertaken to rule out such changes in the transition state with mutant OMP synthases.

When ^{3}k has a value greater than unity, but bound substrate (or product) does not have an opportunity to dissociate before crossing the transition state barrier, the ^{3}k is masked, and not revealed in the observed KIE. This is the situation for WT OMP synthase. Isotope trapping experiments confirm that commitments for bound OMP and PRPP are high (21). In WT, KIE values for reverse catalysis were measurable when a slowly utilized PP_i analog was employed, but with the two natural substrates OMP and PP_i, KIE values were near one. This masking effect arises from the sequestered active site that results from loop closing. As a labeled substrate molecule encounters the barrier, and fails to cross it, it remains bound in the loop-closed state until eventual crossing.

In this context, the E107A enzyme provided predictable KIE data. The residue makes two side chain hydrogen bonds (to Lys103 and Lys73) in the loop-closed structure that appear to help close the loop successfully. In the absence of these bonds, the transition state barrier for chemistry may be higher, and loop opening and substrate dissociation may be faster,

lowering commitment factors. In keeping with these expectations, the [1-^{3}H]OMP and PRPP KIE values are higher than WT. The case of H105A is also interesting. The structure (1) suggests that His105 only makes one side chain hydrogen bond in the closed complex, that to PRPP. In each direction a burst of product formation was noted, showing that on-enzyme chemistry occurs with rate constants close to WT (Figure 3; data for reverse reaction not shown). However, this mutant shows high KIE values in the forward and reverse reactions, and thus very low apparent commitments. Thus, a label-bearing substrate molecule explores the transition state barrier, fails to cross it, and by dissociation is discriminated against.

It is more difficult to explain the behavior of other mutant OMP synthases. In essence, when the chemical transition state is able to equilibrate with dissociated substrate, intrinsic values should be fully expressed. For K103A this does not seem to be the case. Since the on-enzyme conversion of E•MgPRPP•orotate to E•OMP•$MgPP_i$ was shown to be slow, and K_D values for OMP and PRPP are slightly elevated, we would expect that observed KIE values would be high. Instead, they are well below those seen with H105A, and close to unity for Δ102Δ106. Taking K103A, if we accept the reasonable assumption that bound substrates can escape the active site of the ternary substrate complexes minimally at the rate of WT (20 and 80 s^{-1} for PRPP and OMP respectively, *21*), and that on-enzyme chemistry proceeds at 0.05 s^{-1}, the ^{3}k should be fully expressed. If we follow the assumption that ^{3}k is not greatly altered, we must then assume that substrate complexes exploring the transition state barrier are not in equilibrium with the free substrate. It may be that loop-closed complexes of Lys103 or Δ102Δ106 can achieve chemistry at reasonable rates, but that these competent complexes form only rarely. This could occur if a dominant role for Lys103 is to guide the flexible loop into a catalytically competent position, so that the apparent slow enzyme chemistry of K103A ternary substrate complexes is in fact a result of very infrequent successful loop movement. In comparing WT and K103A or Δ102Δ106 it is not unlikely that the barriers for successful loop closure are higher for the mutants than for WT. However, we need also to assume that the barrier to the chemical transition state is relatively low within loop-closed complexes, which is not appealing, since Lys103 clearly makes a number of important hydrogen bonds. We also need to assume that the barrier to loop re-opening is high within complexes that are exploring the transition state barrier, so that such complexes do not dissociate before they cross the transition state barrier. Solutions of the structures for loop-closed complexes of these mutants may be valuable in understanding the origin of these unexpected KIE results.

Acknowledgments

We thank Vern L. Schramm for helpful advice. Most of the KIE work was performed by Bradley A. Bizzle.

References

1. Grubmeyer C, Hansen MR, Fedorov AA, Almo SC. preceding paper.
2. Scapin G, Grubmeyer C, Sacchettini JC. Crystal structure of orotate phosphoribosyltransferase. Biochemistry. 1994; 33:1287–1294. [PubMed: 8312245]
3. Scapin G, Ozturk DH, Grubmeyer C, Sacchettini JC. The crystal structure of the orotate phosphoribosyltransferase complexed with orotate and alpha-D-5-phosphoribosyl-1-pyrophosphate. Biochemistry. 1995; 34:10744–10754. [PubMed: 7545004]
4. Henriksen A, Aghajari N, Jensen KF, Gajhede M. A flexible loop at the dimer interface is a part of the active site of the adjacent monomer of *Escherichia coli* orotate phosphoribosyltransferase. Biochemistry. 1996; 35:3803–3809. [PubMed: 8620002]

5. Ozturk DH, Dorfman RH, Scapin G, Sacchettini JC, Grubmeyer C. Structure and function of *Salmonella typhimurium* orotate phosphoribosyltransferase: protein complementation reveals shared active sites. Biochemistry. 1995; 34:10764–10770. [PubMed: 7545006]
6. González-Segura L, McClard RW, Hurley TD. Ternary complex formation and induced asymmetry in orotate phosphoribosyltransferase. Biochemistry. 2007; 46:14075–14086. [PubMed: 18020427]
7. Wang GP, Cahill SM, Liu X, Girvin ME, Grubmeyer C. Motional dynamics of the catalytic loop in OMP synthase. Biochemistry. 1999; 38:284–295. [PubMed: 9890909]
8. Callender R, Dyer RB. Advances in time-resolved approaches to study the dynamical nature of enzyme catalysis. Chem Rev. 2006; 106:3031–3042. [PubMed: 16895316]
9. Pompliano DL, Peyman A, Knowles JR. Stabilization of a reaction intermediate as a catalytic device: definition of the functional role of the flexible loop in triosephosphate isomerase. Biochemistry. 1990; 29:3186–3194. [PubMed: 2185832]
10. Williams JC, McDermott AE. Dynamics of the flexible loop of triosephosphate isomerase: the loop motion is not ligand gated. Biochemistry. 1995; 34:8309–8319. [PubMed: 7599123]
11. Smith JL. Glutamine PRPP amidotransferase: snapshots of an enzyme in action. Current Opinion in Structural Biology. 1998; 8:686–694. [PubMed: 9914248]
12. Shi W, Li CM, Tyler PC, Furneaux RH, Grubmeyer C, Schramm VL, Almo SC. The 2.0 Å structure of human hypoxanthine-guanine phosphoribosyl-transferase in complex with a transition-state analog inhibitor. Nature Struct Biol. 1999; 6:588–593. [PubMed: 10360366]
13. Ozturk DH, Dorfman RH, Scapin G, Sacchettini JC, Grubmeyer C. Locations and functional roles of conserved lysine residues in *Salmonella typhimurium* orotate phosphoribosyltransferase. Biochemistry. 1995; 34:10755–10763. [PubMed: 7545005]
14. Dawson, RMC.; Elliott, DC.; Elliott, WH.; Jones, KM. Data for Biochemical Research. 3rd. Oxford Science Publications; Oxford: 1986.
15. Tao W, Grubmeyer C, Blanchard JS. Transition state structure of *Salmonella typhimurium* orotate phosphoribosyltransferase. Biochemistry. 1996; 35:14–21. [PubMed: 8555167]
16. Zhang Y, Luo M, Schramm VL. Transition states of *Plasmodium falciparum* and human orotate phosphoribosyltransferases. J Am Chem Soc. 2009; 131:4685–4694. [PubMed: 19292447]
17. Wang F, Shi W, Nieves E, Angeletti RH, Schramm VL, Grubmeyer C. A transition-state analogue reduces protein dynamics in hypoxanthine-guanine phosphoribosyltransferase. Biochemistry. 2001; 40:8043–8054. [PubMed: 11434773]
18. Ramaswamy S, Park DH, Plapp BV. Substitutions in a flexible loop of horse liver alcohol dehydrogenase hinder the conformational change and unmask hydrogen transfer. Biochemistry. 1999; 38:13951–13959. [PubMed: 10529241]
19. Miller GP, Wahnon DC, Benkovic SJ. Interloop contacts modulate ligand cycling during catalysis by *Escherichia coli* dihydrofolate reductase. Biochemistry. 2001; 40:867–875. [PubMed: 11170407]
20. Bhabha G, Lee J, Ekiert DC, Gam J, Wilson IA, Dyson HJ, Benkovic SJ, Wright PE. A dynamic knockout reveals that conformational fluctuations influence the chemical step of enzyme catalysis. Science. 2011; 332:234–238. [PubMed: 21474759]
21. Wang GP, Lundegaard C, Jensen KF, Grubmeyer C. Kinetic mechanism of OMP synthase: a slow physical step following group transfer limits catalytic rate. Biochemistry. 1999; 38:275–283. [PubMed: 9890908]
22. Xu Y, Eads JC, Sacchettini JC, Grubmeyer C. Kinetic mechanism of human hypoxanthine-guanine phosphoribosyltransferase: rapid phosphoribosyl transfer chemistry. Biochemistry. 1997; 36:3700–3712. [PubMed: 9132023]
23. Li, C. Ph D Thesis. Albert Einstein College of Medicine; 1999. Transition State Inhibitors of 6-Oxopurine Phosphoribosyltransferases.
24. Ho SN, Hunt HD, Horton RM, Pullen JK, Pease LR. Site-directed mutagenesis by overlap extension using the polymerase chain reaction. Gene. 1989; 77:51–59. [PubMed: 2744487]
25. Bhatia M, Vinitsky A, Grubmeyer C. Kinetic mechanism of orotate phosphoribosyltransferase from *Salmonella typhimurium*. Biochemistry. 1990; 29:10480–10487. [PubMed: 2271660]
26. Grubmeyer C, Segura E, Dorfman R. Active site lysines in orotate phosphoribosyltransferase. J Biol Chem. 1993; 268:20299–20304. [PubMed: 8376388]

27. Penefsky HS. A centrifuged-column procedure for the measurement of ligand binding by beef heart F1. Methods Enzymol. 1979; 56:527–530. [PubMed: 156867]
28. Scapin G, Sacchettini JC, Dessen A, Bhatia M, Grubmeyer C. Primary structure and crystallization of orotate phosphoribosyltransferase from *Salmonella typhimurium*. J Mol Biol. 1993; 230:1304–1308. [PubMed: 8487307]
29. Parkin, DW. Methods for the determination of competitive and noncompetitive kinetic isotope effects. In: Cook, PF., editor. Enzyme Mechanism from Isotope Effects. CRC Press; 1991. p. 269-290.
30. Cunningham BC, Wells JA. High-resolution epitope mapping of hGH-receptor interactions by alanine-scanning mutagenesis. Science. 1989; 244:1081–1085. [PubMed: 2471267]
31. Cleland WW. The use of isotope effects to determine transition-state structures for enzymic reactions. Methods Enzymol. 1982; 87:625–641. [PubMed: 7176928]
32. Fedorov A, Shi W, Kicska G, Fedorov E, Tyler PC, Furneaux RH, Hanson JC, Gainsford GJ, Larese JZ, Schramm VL, Almo SC. Transition state structure of purine nucleoside phosphorylase and principles of atomic motion in enzymatic catalysis. Biochemistry. 2001; 40:853–860. [PubMed: 11170405]
33. Luo M, Li L, Schramm VL. Remote mutations alter transition-state structure of human purine nucleoside phosphorylase. Biochemistry. 2008; 47:2565–2576. [PubMed: 18281957]
34. Bruice TC, Benkovic SJ. Chemical basis for enzyme catalysis. Biochemistry. 2000; 39:6267–6274. [PubMed: 10828939]
35. Northrop, DB. Intrinsic isotope effects in enzyme-catalyzed reactions. In: Cook, PF., editor. Enzyme Mechanism from Isotope Effects. CRC Press; Florida: 1991. p. 181-202.

Abbreviations

OMP synthase	orotate phosphoribosyltransferase
WT	wild-type enzyme
OMP	orotidine 5′-monophosphate
KIE	kinetic isotope effect
GPAT	glutamine PRPP amidotransferase
HGPRTase	hypoxanthine-guanine phosphoribosyltransferase
TIM	triose phosphate isomerase
PRPP	5-phosphoribosyl-1-pyrophosphate

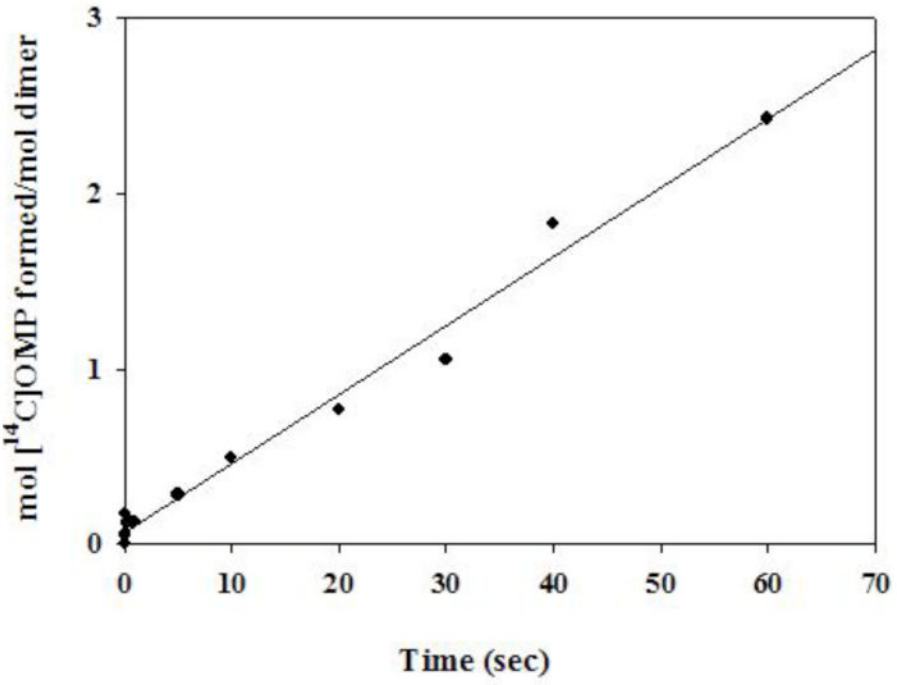

Figure 1.

Rate of product formation for K103A in the forward phosphoribosyltransferase reaction at 22°C. The chemical quench study was conducted as described in Materials and Methods. The reaction mixture contained 1014 μM [2-^{14}C]orotate, 6 mM PRPP, 12 mM $MgCl_2$, and 45 μM K103A mutant enzyme in 80 mM Tris-Cl, pH 8.0. No burst of product formation was observed. The calculated steady-state rate was 0.02 s^{-1} (see text). Note that the y-axis represents catalysis on a per dimer basis.

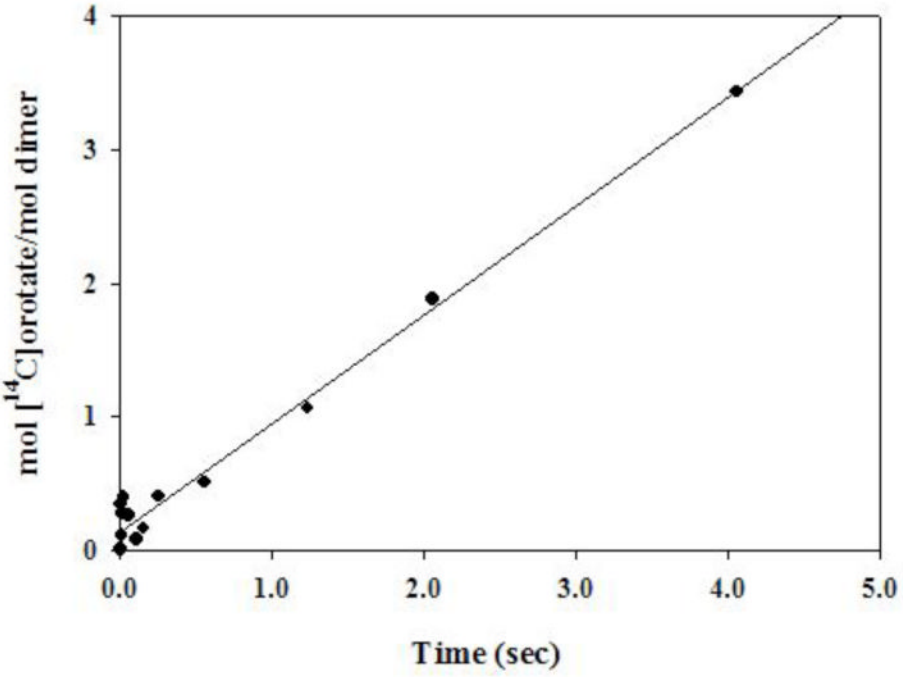

Figure 2.

Rate of product formation for the E107A mutant in the reverse pyrophosphorolysis reaction at 22°C. The chemical quench study was conducted as described in Materials and Methods. The reaction mixture contained 300 μM [^{14}C]OMP, 2 mM PP_i, 3 mM $MgCl_2$, and 30 μM E107A mutant enzyme in 80 mM Tris-Cl, pH 8.0. No burst of product formation was observed. The calculated steady-state rate was 0.4 s^{-1} (see text). Note that the y-axis represents catalysis on a per dimer basis.

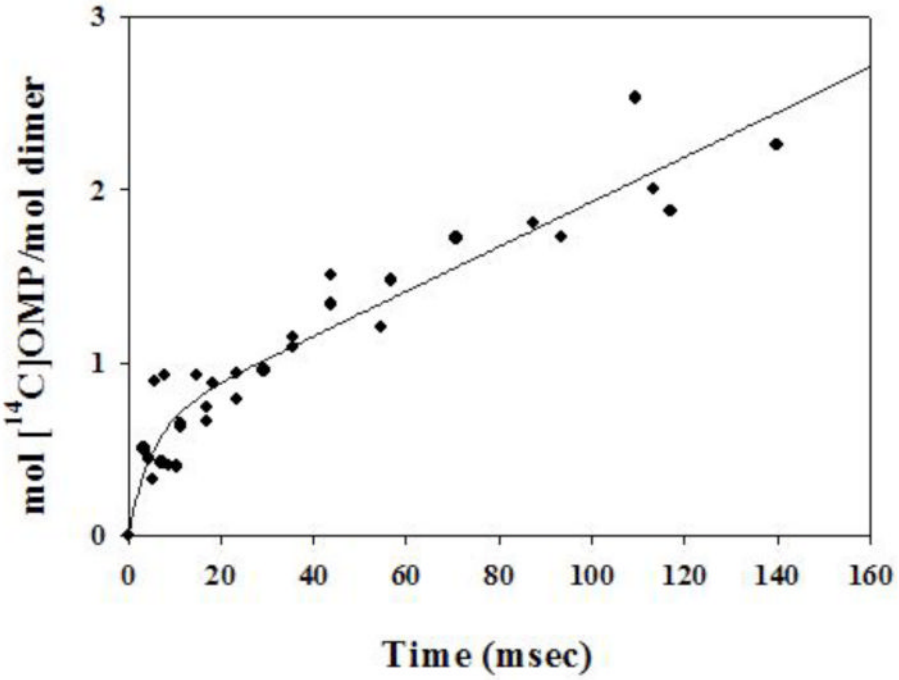

Figure 3.

Rate of product formation for the H105A mutant in the forward phosphoribosyltransferase reaction at 22°C. The reaction mixture contained 405 μM [2-^{14}C]orotate, 2 mM PRPP, 6 mM $MgCl_2$, and 40.5 μM H105A mutant enzyme in 80 mM Tris-Cl, pH 8.0. A burst of product formation followed by a steady-state phase was observed. The data were fit to the equation $y = N \times (1\text{-}e^{-kobs \times t}) + kt$ (using SigmaPlot (SPSS, Inc). The burst phase was fit to a rate (k_{obs}) of 200 s^{-1} . The magnitude of the burst (N) was 0.64 mol [^{14}C]OMP/mol dimer. The calculated steady-state rate (6.4 s^{-1}) was comparable to the value of k_{cat} obtained at 30°C (5.3 s^{-1}) from spectrophotometric measurements. Note that the y-axis represents catalysis on a per dimer basis.

Table 1

Oligonucleotide primers for the site-directed mutagenesis procedure.

Mutant	Mutagenic Primer
E101A	5′ CCGCAAAGCGGCAAAAGATCATG 3′
	5′ CTTTTGCCGCTTTGCGGTTAAAG 3′
D104A	5′ GGCAAAAGCTCATGGTGAAGGC 3′
	5′ CACCATGAGCTTTTGCCTCTTTG 3′
H105A	5′ CAAAAGATGCTGGTGAAGGCGG 3′
	5′ CTTCACCAGCATCTTTTGCCTCT 3′
G106A	5′ AGATCATGCTGAAGGCGGGAGC 3′
	5′ CGCCTTCAGCATGATCTTTTGCC 3′
E107A	5′ TCATGGTGCAGGCGGGAGCCT 3′
	5′ TCCCGCCTGCACCATGATCTTTT 3′
G108A	5′ ATGGTGAAGCCGGGAGCCT 3′
	5′ GGCTCCCGGCTTCACCATGA 3′
G109A	5′ AAGGCGCGAGCCTGGTGGG 3′
	5′ AGGCTCGCGCCTTCACCATG 3′
Δ102Δ106	5′ AAGAGAAAGATCATGAAGGCGGGA 3′
	5′ CCTTCATGATCTTTCTCTTTGCGG 3′
5′ flanking primer	5′ GCGAATCCATATGAAACCGTATC 3′
3′ flanking primer	5′ CCGGCAGGATCCGCTTACAC 3′

Table 2

Steady-state kinetic parameters of catalytic loop mutants of *S. typhimurium* OMP synthase at 30°C in the forward phosphoribosyltransferase reaction.

			PRPP		Orotate
Enzyme	**k_{cat} (s^{-1})**	**K_M (μM)**	**k_{cat}/K_M (mM^{-1} s^{-1})**	**K_M (μM)**	**k_{cat}/K_M (mM^{-1} s^{-1})**
WT	56 ± 2.5	18 ± 5	3100	19 ± 3	3000
K100A[a]	12 ± 0.2	179 ± 11	64	72 ± 4	160
E101A	72 ± 4.5	26 ± 4	2750	62 ± 11	1150
K103A[a]	0.05 ± 0.002	285 ± 4	0.2	42 ± 3	1
D104A	64 ± 2.5	42 ± 6	1500	26 ± 4	2500
H105A	5.3 ± 0.8	66 ± 8	80	179 ± 10	30
G106A	57 ± 1.5	38 ± 7	1500	87 ± 6	650
E107A	2.4 ± 0.3	6 ± 3	420	380 ± 100	6
G109A	28 ± 2.0	42 ± 10	670	137 ± 26	205

For the calculation of k_{cat}, the subunit Mr was employed.

[a]Data from (13).

Table 3

Steady-state kinetic parameters of catalytic loop mutants of *S. typhimurium* OMP synthase at 30°C in the reverse pyrophosphorolysis reaction.

	OMP			PP_i	
Enzyme	**k_{cat} (s^{-1})**	**K_M (μM)**	**k_{cat}/K_M (mM^{-1} s^{-1})**	**K_M (μM)**	**k_{cat}/K_M (mM^{-1} s^{-1})**
WT	18 ± 0.3	3 ± 0.3	5200	31 ± 3	580
K100A[a]	12 ± 0.2	13 ± 1	920	958 ± 40	13
E101A	25 ± 1.8	4 ± 1	7040	86 ± 6	295
K103A[a]	0.05 ± 0.001	20 ± 1	2.5	146 ± 1	0.3
D104A	18 ± 0.5	16 ± 9	1160	28 ± 3	670
H105A	2.2 ± 0.2	7 ± 1	300	822 ± 27	2.6
G106A	17 ± 1.8	11 ± 4	1560	100 ± 11	165
E107A	0.3 ± 0.04	14 ± 6	21	297 ± 76	1
G109A	13 ± 0.7	8 ± 1	1610	627 ± 90	20

For the calculation of k_{cat}, the subunit Mr was employed.

[a]Data from (13).

Table 4

Equilibrium binding constants for selected *S. typhimurium* OMP synthase mutants[a].

	K_D (μM)	
Enzyme	**OMP**	**PRPP**
WT	3 ± 0.1	33 ± 0.5
E101A	12 ± 2	36 ± 3
K103A	3 ± 0.1	125 ± 11
D104A	ND	13 ± 0.7
H105A	4 ± 0.3	92 ± 11
E107A	6.5 ± 0.8	7.1[a] ± 0.5

Experiments performed in 80 mM Tris-Cl, pH 8.

[a]Stoichiometry (n) was close to 1 mol ligand per mole subunit for all enzymes.

[b]Experiment performed in 80 mM Na-Tricine, pH 8.

ND: not determined

Table 5

Equilibrium binding constants for WT *S. typhimurium* OMP synthase and the loop deletant Δ102Δ106.

	WT enzyme		**Δ102Δ106**	
Ligand	K_D (μM)	n[a]	K_D (μM)	n[a]
Orotate	280 ± 30	0.90	340 ± 50	0.71
PRPP	33 ± 0.5	0.85	80 ± 17	0.90
OMP	3.1 ± 0.1	0.90	2.0 ± 0.1	0.75
PP_i[b]	960 ± 120	0.86	900 ± 300	0.66

[a]Expressed as mol of ligand bound per mol subunit. Values ± 10%.

[b]Values were extrapolated from Scatchard plots due to weak binding.

Table 6

(1′-^{3}H) Kinetic Isotope Effects on *S. typhimurium* Mutant OMP synthases[a].

Enzyme	Forward		Reverse	
	k_{cat}/K_M PRPP (fold decrease)[b]	KIE	k_{cat}/K_M OMP (fold decrease)[c]	KIE
WT	(1)	1.019 ± 0.0069	(1)	1.059 ± 0.0038
E101A	1.1	1.016 ± 0.0025	0.74	1.155 ± 0.0064
K103A	15500	1.020 ± 0.0079	2080	1.095 ± 0.013
D104A	2.1	1.012 ± 0.0031	4.5	1.026 ± 0.0095
H105A	39	1.136 ± 0.0071	17	1.210 ± 0.0050
G106A	2.1	1.057 ± 0.0138	3.4	1.057 ± 0.0043
E107A	7.4	1.111 ± 0.0038	248	1.179 ± 0.0049
G109A	4.6	1.118 ± 0.0074	3.3	1.153 ± 0.0028

[a] Kinetic isotope effects for the forward direction with [1-^{3}H]PRPP and for the reverse reaction with [1′-^{3}H]OMP were measured as described in Methods.

[b] From Table 2.

[c] From Table 3